JOURNAL OF IRON AND STEEL RESEARCH, INTERNATIONAL. 2010, 17(9): 14-18

# Fluid Flow and Heat Transfer Modeling of AC Arc in Ferrosilicon Submerged Arc Furnace

M Mohebi Moghadam[1], S H Seyedein[2], M Reza Aboutalebi[3]
(School of Metallurgy and Materials Engineering, Iran University of Science and Technology, Tehran 16846-13114, Iran)

**Abstract**: A two-dimensional mathematical model was developed to describe the heat transfer and fluid flow in an AC arc zone of a ferrosilicon submerged arc furnace. In this model, the time-dependent conservation equations of mass, momentum, and energy in the specified domain of plasma zone were numerically solved by coupling with the Maxwell and Laplace equations for magnetic filed and electric potential, respectively. A control volume-based finite difference method was used to solve the governing equations in cylindrical coordinates. The reliability of the developed model was checked by experimental data from the previous available literature. The results of present model were in good agreement with the given data comparing with other models, because of solving the Maxwell and Laplace equations simultaneously in order to calculate current density. In addition, parametric studies were carried out to evaluate the effects of electrical current and arc length on flow field and temperature distribution within the arc. According to the computed results, a lower power input led to a higher arc efficiency.

**Key words**: plasma modeling; heat transfer; fluid flow; AC submerged arc furnace

In the ferrosilicon submerged arc furnace, heat is supplied to the molten bath by electric arc through graphite electrodes. In this regard, fundamental understanding of the heat transfer, fluid flow, and electromagnetic phenomena is necessary to improve the control of these metallurgical reactors[1]. To achieve this goal, use of computational fluid dynamic (CFD) models has been increasingly popular. In 1981, Ushio and Szekely firstly and then McKelliget and Szekely performed numerical simulation of a DC electric arc furnace by using the turbulent Navier-Stokes, energy conservation and Maxwell equations in the arc and bath regions of the system. In their calculation, a parabolic current density distribution was assumed through the arc region to simplify the magnetic problem. In 1985, McKelliget and Szekely used the magnetic diffusion equation to predict heat transfer and fluid flow in a welding arc. With more powerful computers, it became possible to solve more complex problems. In 1992, Choo, Szekely and Westhof, and in 1995, Qian, Farouk and Matharasan, solved Laplace's equation for the electric potential to determine boundary conditions for a model of the weld pool. In 1996, Larsen and Bakken used the magnetic transport equation to predict the current and magnetic field in an AC arc[2].

As mentioned above, several individual models of DC electric arcs in welding or furnace were developed. However, in the AC electric arc furnace, which has a great share in metallurgical industry, very limited researches have been done[3].

Therefore, the present work was undertaken to develop a model of AC arc to predict temperature distribution, flow pattern, and current density on the melt surface. This information was further used to define boundary condition and represent heating and mixing effects on the metal bath. For testing the reliability of the model, predicted velocities and temperatures were compared with experimental data from Bowman's investigation. These results showed good consistency and confirmed that the model prediction is reliable[4-5].

## 1 Mathmatical Model

The schematic drawing of the studied domain is given in Fig. 1. As shown, the domain is restricted

**Biography**: M Mohebi Moghadam(1980—), Male, Master; **E-mail**: Mahyar. mm@gmail. com; **Received Date**: December 1, 2008

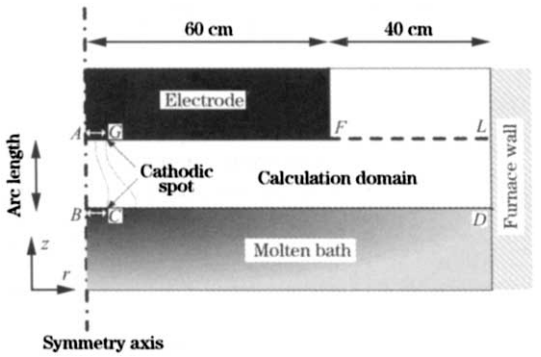


**Fig. 1 Calculation domain for AC arc model**

between graphite electrode and molten bath from top and bottom and central electrode axis and furnace wall from left and right.

In present model, the arc was considered as a fluid with temperature dependent properties[6-10]. Likewise, the following assumptions were made to governing the equations:

1) The arc is axis symmetric[11].

2) The operation of the arc is time dependent, i. e. unsteady state[11].

3) The arc is local thermal equilibrium (LTE), i. e. the electron and heavy particle temperature are similar[11-12].

4) The radiation flux is calculated in optically thin condition[12-14].

5) The surface of the furnace wall, electrode bottom, and molten is flat[2,11].

### 1.1 Transport equations for AC arc

The governing time-dependent transport equations for AC arc have been expressed in two-dimensional cylindrical coordinates.

1) Mass conservation

$$\frac{\partial \rho}{\partial t}+\frac{1}{r}\frac{\partial}{\partial r}(r\rho v)+\frac{\partial}{\partial z}(\rho u)=0 \tag{1}$$

where, $\rho$ is the density; $t$ is the time; $r$ is the radial distance; and $z$ is the axial distance; $v$ and $u$ are the velocity components in the radial and axial directions, respectively[6].

2) Conservation of axial momentum

$$\frac{\partial(\rho u)}{\partial t}+\frac{1}{r}\frac{\partial}{\partial r}(r\rho vu)+\frac{\partial}{\partial z}(\rho uu)=-\frac{\partial p}{\partial z}+\frac{\partial}{\partial z}\left[2\mu\frac{\partial u}{\partial z}\right]+\frac{1}{r}\frac{\partial}{\partial r}\left[r\mu\left(\frac{\partial v}{\partial z}+\frac{\partial u}{\partial r}\right)\right]+j_rB_\theta \tag{2}$$

where, $\mu$ is the viscosity; $p$ is the static pressure; $j_r$ is the current density in radial direction; and $B_\theta$ is the magnetic flux density in the azimuthal direction. The product $j_rB_\theta$ is the axial component of the Lorentz force produced by current and induced magnetic flux density in the solution domain[6].

3) Conservation of radial momentum

$$\frac{\partial(\rho v)}{\partial t}+\frac{1}{r}\frac{\partial}{\partial r}(r\rho vv)+\frac{\partial}{\partial z}(\rho uv)=-\frac{\partial p}{\partial r}+\frac{2}{r}\cdot\frac{\partial}{\partial r}\left[r\mu\frac{\partial v}{\partial r}\right]+\frac{\partial}{\partial z}\left[\mu\left(\frac{\partial v}{\partial z}+\frac{\partial u}{\partial r}\right)\right]-\frac{2\mu v}{r^2}-j_zB_\theta \tag{3}$$

where, $j_z$ is the current density in axial direction; and the product $j_zB_\theta$ is the radial component of the Lorentz force[6].

4) Conservation of thermal energy

$$\frac{\partial(\rho h)}{\partial t}+\frac{1}{r}\frac{\partial}{\partial r}(r\rho vh)+\frac{\partial}{\partial z}(\rho uh)=\frac{\partial}{\partial z}\left[\frac{k}{c_p}\frac{\partial h}{\partial z}\right]+\frac{1}{r}\cdot\frac{\partial}{\partial r}\left[r\frac{k}{c_p}\frac{\partial h}{\partial r}\right]+\frac{j_z^2+j_r^2}{\sigma}+\frac{5k_B}{2e}\left[\frac{j_z}{c_p}\frac{\partial h}{\partial z}+\frac{j_r}{c_p}\frac{\partial h}{\partial r}\right]-S_r \tag{4}$$

where, $h$ is the enthalpy; $c_p$ is the specific heat at constant pressure; $k$ is the thermal conductivity; $\sigma$ is the electrical conductivity; $S_r$ is the radiation loss term; $k_B$ is the Boltzmann constant; and $e$ is the electron charge[6].

5) Magnetic transport equation

$$\frac{\partial B_\theta}{\partial t}+\frac{1}{r}\frac{\partial}{\partial r}(rvB_\theta)+\frac{\partial}{\partial z}(uB_\theta)=\frac{\partial}{\partial r}\left[\frac{\Gamma_m}{r}\frac{\partial}{\partial r}(rB_\theta)\right]+\frac{\partial}{\partial z}\left[\Gamma_m\frac{\partial B_\theta}{\partial z}\right] \tag{5}$$

where, $\Gamma_m$ is the magnetic diffusivity, which governs the diffusion of AC magnetic field through the arc plasma, and $\Gamma_m=(\sigma\mu_0)^{-1}$; and $\mu_0$ is the vacuum permeability[6,11].

6) Electric potential equation

$$\frac{\partial}{\partial z}\left[\sigma\frac{\partial \varphi}{\partial z}\right]+\frac{1}{r}\frac{\partial}{\partial r}\left[\sigma r\frac{\partial \varphi}{\partial r}\right]=0 \tag{6}$$

where, $\varphi$ is the electrical potential.

### 1.2 Boundary conditions for AC arc

To solve the transport equations in the calculation domain, boundary conditions should be specified. A complete listing of boundary conditions for the AC arc is presented in Table 1.

Symmetry conditions are used along the axis $AB$. No slip condition is applied for all walls. The temperature on the crater wall, molten surface, and electrode (excluding cathode spot) is fixed to 2000 K. The following parabolic current density distribution is assumed on the cathode spot[2].

$$j_z=2j_c\left[1-\left(\frac{r}{R_c}\right)^2\right] \tag{7}$$

where

$$j_c=I/(\pi R_c^2) \tag{8}$$

**Table 1 Boundary conditions for AC arc**

| | *AB* | *BC* | *CD* | *DL* | *LF* | *FG* | *GA* |
|---|---|---|---|---|---|---|---|
| $v$ | $v=0$ | $v=0$ | $v=0$ | $v=0$ | $v=0$ | $v=0$ | $v=0$ |
| $u$ | $\frac{\partial u}{\partial r}=0$ | $u=0$ | $u=0$ | $u=0$ | $\frac{\partial u}{\partial z}=0$ | $u=0$ | $u=0$ |
| $h$ | $\frac{\partial h}{\partial r}=0$ | $T=2000$ K | $T=2000$ K | $T=2000$ K | $\frac{\partial h}{\partial z}=0$ | $T=2000$ K | $T=4000$ K |
| $B_\theta$ | $B_\theta=0$ | Anodic period $\frac{\partial B_\theta}{\partial z}=0$ Cathodic period $B_\theta=\frac{\mu_0 j_c r}{2}$ | Anodic period $\frac{\partial B_\theta}{\partial z}=0$ Cathodic period $B_\theta=\frac{\mu_0 I}{2\pi r}$ | $B_\theta=\frac{\mu_0 I}{2\pi r}$ | Cathodic period $B_\theta=\frac{\mu_0 I}{2\pi r}$ Anodic period $\frac{\partial B_\theta}{\partial z}=0$ | Cathodic period $B_\theta=\frac{\mu_0 I}{2\pi r}$ Anodic period $\frac{\partial B_\theta}{\partial z}=0$ | Cathodic period $B_\theta=\frac{\mu_0 j_c r}{2}$ Anodic period $\frac{\partial B_\theta}{\partial z}=0$ |
| $\varphi$ | $\frac{\partial \varphi}{\partial r}=0$ | Anodic period $\varphi=0$ Cathodic period $\frac{\partial \varphi}{\partial z}=\frac{j_z}{\sigma}$ | Anodic period $\varphi=0$ Cathodic period $\frac{\partial \varphi}{\partial z}=0$ | $\frac{\partial \varphi}{\partial r}=0$ | Cathodic period $\frac{\partial \varphi}{\partial z}=0$ Anodic period $\varphi=0$ | Cathodic period $\frac{\partial \varphi}{\partial z}=0$ Anodic period $\varphi=0$ | Cathodic period $\frac{\partial \varphi}{\partial z}=\frac{j_z}{\sigma}$ Anodic period $\varphi=0$ |

$I$ is the applied electrical current; and $R_c$ is the radius of cathodic spot. Since the cathode alternates between the graphite electrode and the melt surface subsequently, the boundary conditions of magnetic field and electrical potential are changed according to the change of the electrical current polarity[6,11].

### 1.3 Solution method

In previous researches, three different methods have been used to determine the Lorentz forces: the Laplace equation, the magnetic diffusion equation, and the complete magnetic transport equation. The first two methods have excluded the induced electric field term from the solution. This assumption could be applied in the case that the magnetic Reynolds number is much less than unity. Under this condition, these methods are given good approximation of the Lorentz force, but this assumption is not acceptable in high current arcs. The third method has included this term; nevertheless, it is not applicable for the calculation of current density from the Ohm's law[10,15]. In the present work, for the first time, the Laplace equation for electric potential and the complete magnetic transport (Maxwell) equation for magnetic field are solved in coupled with momentum and energy equations to overcome these problems. In present solution, Laplace and Maxwell equations predict imposed and induced electromagnetic field in terms of Ohm's law, which were adapted to determine the Lorentz forces[15]:

$$J=\sigma(E+V\times B) \tag{9}$$

where, $E$ is an imposed electrical field that is calculated from $E=-\nabla\varphi$; $V$ is the velocity vector; and $B$ is the vector of magnetic flux density. After providing all terms of Ohm's law, the electrical current density in radial and axial directions could be calculated for all points of the domain[15]. To solve the governing equations, a control volume based finite difference method was used in cylindrical coordinates. Numerical method used for solving equation is TDMA, and CIMPLEC algorithm is used for correcting the relationship between velocity and pressure[16-17].

## 2 Results and Discussion

Since the AC arc is time-dependent, in each period of AC electric current with change in polarity, the shape of temperature distribution and fluid flow are either changed, with respect to the boundary conditions. The temperature distribution and flow pattern in domain with arc length of 10 cm are shown in Fig. 2 and Fig. 3. The electrical current supplied in this case was $I=80000\cos(2\pi\lambda t)$, where $\lambda$ is the frequency of the AC current[11].

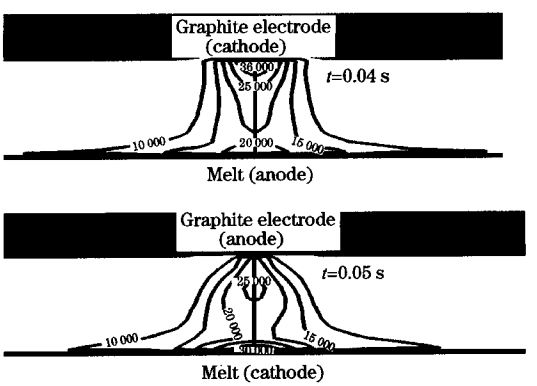


**Fig. 2 Distribution of Kelvin temperature for two kinds of time**

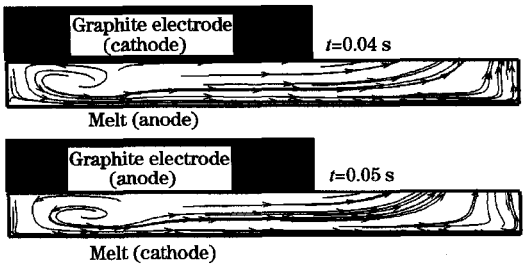


**Fig. 3 Flow pattern for two kinds of time**

To predict the rate of heat transfer between the arc region and the molten bath, current density, temperature and velocity on the melt surface are required. Obtained results by model for different currents and arc lengths are presented in Fig. 4. In all cases, the cathode current density was $1.5\times10^7$ A/m$^2$[6,11].

As expected, increasing the electrical current results in the increase in the velocity and temperature on the melt surface. It can be seen from Fig. 4 that arcs with shorter length show higher temperature

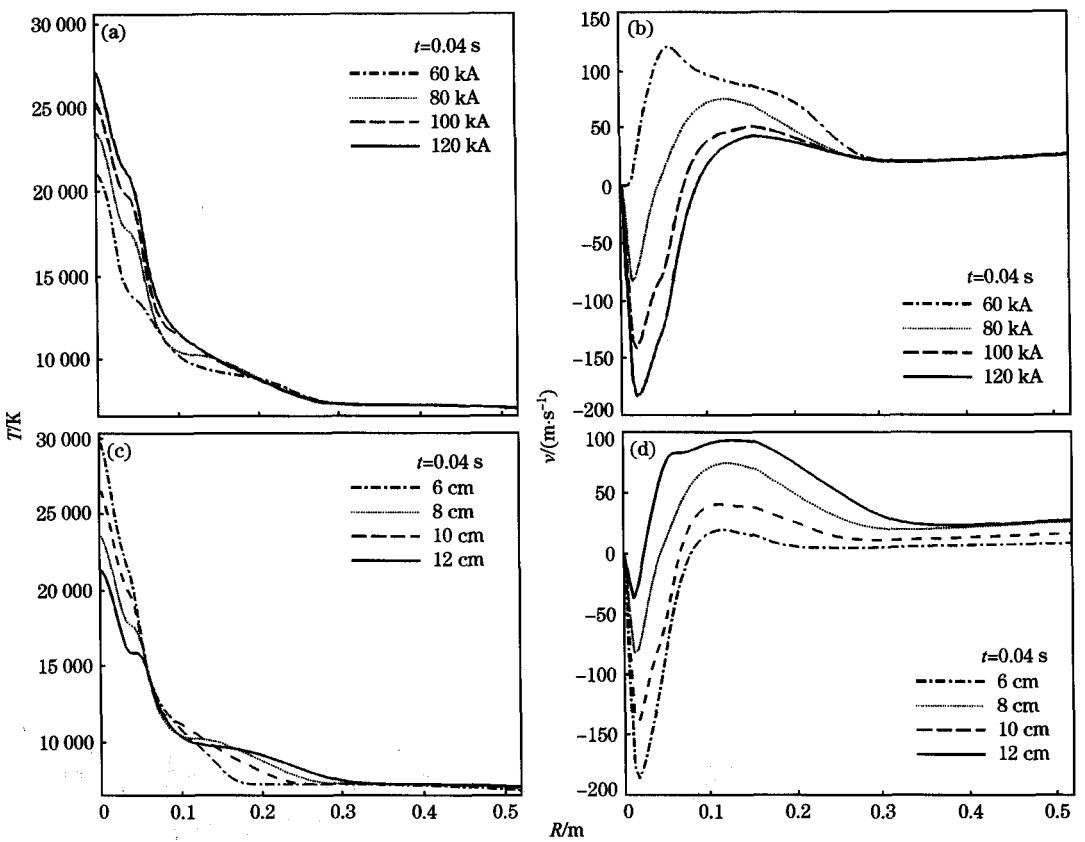


(a), (b) Arc length of 10 cm; (c), (d) Current of 80 kA.

**Fig. 4 Distributions of temperature and radial velocity at melt surface for 0.04 s**

inside the arc column than outside. This subject can be described by radiation term. Although in present diagrams, the results of 60 kA is specified, the current density applied for this case seemed improper.

As mentioned before, the main purpose of this research is to calculate heat transfer from arc to melt surface, which can be used as boundary conditions in molten bath simulations and also in furnace control. Calculation of heat flux in the electric arc is really complicated and included different terms like convection, conduction, radiation, Thompson effect, and condensation of electrons[2,12]. This model by counting all these terms, calculated the heat transfer efficiency of the arc through the molten bath. The efficiency of the arc is defined as heat transfered to the melt divided by the total consumed power. Fig. 5 shows the efficiency of heat transfer from the arc to the molten bath in parametric studies.

As shown in Fig. 5, as long as the arc is stable, the efficiency of heat transfer is increased by reducing electric current. Also, the effect of arc length has an optimum point in arc length of 10 cm. After 10 cm of arc length, the radiation loss is more than the effective heat transfer to melt.

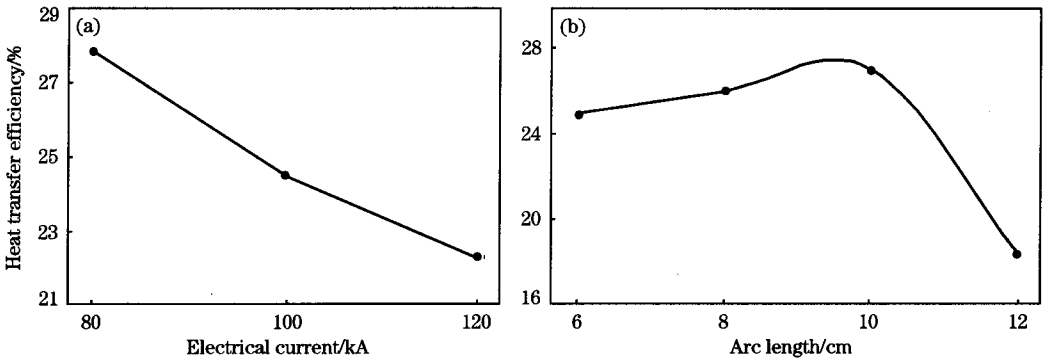


**Fig. 5 Heat transfer efficiency from arc to molten bath for different electrical current (a) and arc length (b)**

## 3 Conclusions

In this study, an AC arc zone in a ferrosilicon submerged furnace is modeled by coupling conservation equations of mass, momentum, and energy with Maxwell and Laplace equations. Solving Maxwell and Laplace equations simultaneously caused an accurate approach to calculating Lorantz force terms in conservation equations for high current AC arcs. Present model makes better prediction from the transport phenomena in AC arc zone and can provide more precise and real data for boundary condition of molten bath simulation in future studies.

This model was used to carry out two parametric studies for different electric currents (60, 80, 100, and 120 kA) and different arc lengths (6, 8, 10, and 12 cm). The predicted results showed that by decreasing the arc currents, the efficiency of heat transfer from arc to molten bath is increased. In addition, according to the results, the optimal arc length in furnace is 10 cm. That means optimization of electric current and arc length is necessary for better operation of submerged arc furnace.

The results of the model also demonstrate that taking the $j_c$ of $1.5\times10^7$ A/m$^2$ in cathodic spot is acceptable for electrical currents greater than 80 kA, but in case with lower input electrical current, the higher electrical current density should be applied.

*The authors wish to acknowledge the Iran Ministry of Mines and Industries for financial support of this project.*

**References:**

[1] Hauksdottir A S, Gestsson A, Vesteinsson A. Submerged-Arc Ferrosilicon Furnace Simulator: Validation for Different Furnaces and Operating Ranges [J]. Control Engineering Practice, 1998, 6(8): 1035.

[2] Alexis J, Ramirez M, Trapaga G, et al. Modeling of a DC Electric Arc Furnace-Heat Transfer From the Arc [J]. ISIJ International, 2000, 40(11): 1089.

[3] Yang Y, Xiao Y, Reuter M A. Analysis of Transport Phenomena in Submerged Arc Furnace for Ferrochrome Production [C] //Gelen H. Proceedings of Tenth International Ferroalloys Congress. Cape Town: SAIMM. 2004: 15.

[4] Bowman B. Effects on Furnace Arcs of Submerging by Slag [J]. Ironmaking and Steelmaking, 1990, 17(2): 123.

[5] Bowman B. Properties of Arcs in DC Furnace [C] //52nd Electric Furnace Conference Proceeding. Nashvile: ISS-AIME, 1994: 111.

[6] Saevarsdottir G A, Bakken J A, Sevastyanenko V G, et al. Modeling of AC Arcs in Submerged-Arc Furnaces for Production of Silicon and Ferrosilicon [J]. Iron and Steelmaker, 2001, 28(10): 51.

[7] Douce A, Delalondere C, Biausser H, et al. Numerical Modeling of an Anodic Metal Bath Heated With an Argon Transferred Arc [J]. ISIJ International, 2003, 43(8): 1128.

[8] Chakraborty B. Principle of Plasma Mechanics [M]. 4th ed. New Delhi: New Age Publisher, 2003.

[9] Obrien R. Plasma Arc Meltworking Processes [M]. New York: American Welding Society, 1967.

[10] Chu S C, Lian S S. Numerical Analysis of Temperature Distribution of Plasma Arc With Molten Pool in Plasma Arc Melting [J]. Computational Material Science, 2004, 30: 441.

[11] Larsen H L, Liping G, Bakken J A. A Numerical Model for the AC Arc in the Silicon Metal Furnace [C] //Tuset, Tveit, Page. INFACON 7. Trondheim: The Norwegian Ferroalloy Organization, 1995: 517.

[12] Goodarzi M, Choo R, Toguri J M. The Effect of the Cathode Tip Angle on the GTAW Arc and Weld Pool: 1. Mathematical Model of the Arc [J]. Applied Physics, 1997, 30(19): 2744.

[13] Reynolds Q. Thermal Radiation Modelling of DC Smelting Furnace Freeboards [J]. Minerals Engineering, 2002, 15 (11): 993.

[14] Guo D, Irons G. Modeling of Radiation Intensity in an EAF [C] //Witt P J, Schwarz M P. Third International Conference on CFD in the Mineral and Process Industries. Melbourne: CSIRO 2003: 223.

[15] Shercliff J A. A Text Book of Magnetohydrodynamics [M]. Oxford: Pergamon Press Ltd, 1965.

[16] Patankar S V. Numerical Heat Transfer and Fluid Flow [M]. Washington D C: Hemisphere Publishing Corporation, 1980.

[17] Bird R B, Stewart W E, Lightfoot E N. Transport Phenomena [M]. 2nd ed. New York: John Wiley and Sons, 2002.